

To Thread or not to Thread: Reaction of Uranyl (UO_2^{2+}) with two Aza-crown Macrocycles**

Gabriella S. Godinho, Kevin K. Lee, Qien Feng, Guang Wu, Justin J. Wilson, and Trevor W.*

*Hayton**

Department of Chemistry and Biochemistry, University of California, Santa Barbara, Santa Barbara, CA
93106, United States

E-mail: hayton@chem.ucsb.edu, justinjwilson@ucsb.edu

**Dedicated to Profs. Peter C. Ford and Galen D. Stucky on the occasion of their retirements.

Abstract

The complexation of the uranyl ion (UO_2^{2+}) by macrocyclic ligands is hindered by the rigidly enforced *trans* orientation of its oxo ligands. To further investigate this coordination chemistry challenge, here we investigate the reactivity of UO_2^{2+} with two different 18-membered aza-crown macrocycles, diaza-dibenzo-18-crown-6 (**DADBC**) and 7,16-bis(*N*-methylacetamide)diaza-18-crown-6 (**BAM**). The reaction of uranyl triflate, $[\text{UO}_2(\text{OTf})_2(\text{THF})_3]$, with **DADBC** in toluene afforded $[\text{UO}_2(\text{DADBC})][\text{OTf}]_2$, in which the UO_2^{2+} ion is fully encapsulated by the macrocycle. This conclusion was supported by NMR, UV-Vis, IR, and Raman spectroscopies, as well as single-crystal X-ray crystallography. Attempts to form the in-macrocycle complex of **BAM**, however, were unsuccessful. The reaction of **BAM** with $[\text{UO}_2(\text{OTf})_2(\text{THF})_3]$ in THF/ CH_2Cl_2 unexpectedly afforded crystals of $[\text{H}_2\text{BAM}][\text{OTf}]_2$, where the protons are derived from solvate water in the **BAM** crystal lattice. In contrast, reaction of **BAM** with $\text{UO}_2(\text{NO}_3)_2 \cdot 6\text{H}_2\text{O}$ resulted in formation of the coordination polymer, $[\text{UO}_2(\kappa^2\text{-NO}_3)_2(\mu\text{-BAM})]_\infty$. The crystal structure of this compound revealed that the **BAM** ligand is coordinated to UO_2^{2+} via its pendent carboxamide donors, while the donor atoms within the macrocyclic cavity remained unbound. The X-ray crystal structure of the free **BAM** ligand was also obtained, which showed that it exists in an identical conformation to that seen in the structure of $[\text{UO}_2(\kappa^2\text{-NO}_3)_2(\mu\text{-BAM})]_\infty$, where the pendent carboxamide donors are engaged in an intramolecular hydrogen-bonding interaction with the donor atoms within the macrocycle. These results suggest that the enthalpic penalty of breaking these intramolecular hydrogen bonds prevents UO_2^{2+} from “threading the needle.” In contrast, **DADBC**, which lacks such intramolecular hydrogen-bonding interactions, can readily accommodate UO_2^{2+} . This comparison demonstrates how subtle modifications to the macrocycle, such as cavity size, rigidity, and pendant donor groups, can affect its affinity for UO_2^{2+} , and provide insights into approaches for macrocycle chelator design for this ion for applications in separations, medicine, and energy.

Introduction

Macrocyclic binding to uranyl (UO_2^{2+}) is complicated by the rigidly *trans* arrangement of its two oxo ligands, which restricts the macrocycle donor atoms to the equatorial plane. This imposition results in strict thermodynamic and kinetic restrictions to ligand binding. In many cases, the binding cavity of the macrocycle is too small to accommodate the linear uranyl ion, while side-on binding is disfavored because of the high $\text{O}_{\text{yl}}-\text{U}-\text{O}_{\text{yl}}$ bending energy.^[1-2] In addition, the need to contort the macrocycle into a planar configuration can result in large kinetic barriers for uranyl binding. As a result of these complications, the first structurally-authenticated example of a macrocyclic ligand coordinating uranyl within its binding cavity was only reported in 1984, namely, $[\text{UO}_2(\text{dicyclohexyl-18-crown-6})]^{2+}$.^[3] Since then, a variety of macrocycles have been found to accommodate uranyl within their binding pockets,^[4] including crown ethers,^[5-11] aza-crown ethers,^[12-13] calixarenes,^[14] thiacalixarenes,^[15-16] expanded porphyrins,^[17-24] hybrid Schiff base/polypyrrolide macrocycles,^[25-35] and hybrid Schiff base/crown ether macrocycles.^[36-38] In many of these cases, the macrocycle fully encapsulates the uranyl ion, occupying all of the equatorial coordination sites (i.e., “threading the needle”). Several of these complexes have also been investigated by computational methods.^[39-44]

However, macrocycles do not always thread the needle.^[45-46] Smaller macrocycles, such as 12-crown-4, 15-crown-5, 2,11-diaza[3,3](2,6)pyridinophane, dibenzotetramethyltetraaza[14]annulene, *p*-*t*Bu-calix[4]arene,^[16] and Me_8 -calix[4]pyrrole cannot accommodate uranyl,^[1, 47-55] presumably because their binding pockets are too small. Additionally, macrocyclic ligands do not readily displace Cl^- , Br^- , or NO_3^- from the uranyl equatorial plane, adding another complication to the synthesis of uranyl macrocycle complexes.^[9, 56-58] Despite these synthetic challenges, macrocyclic ligands have potential applications in uranyl molecular recognition as well as solvent extraction,^[4, 11, 23] motivating researchers to further explore this topic.

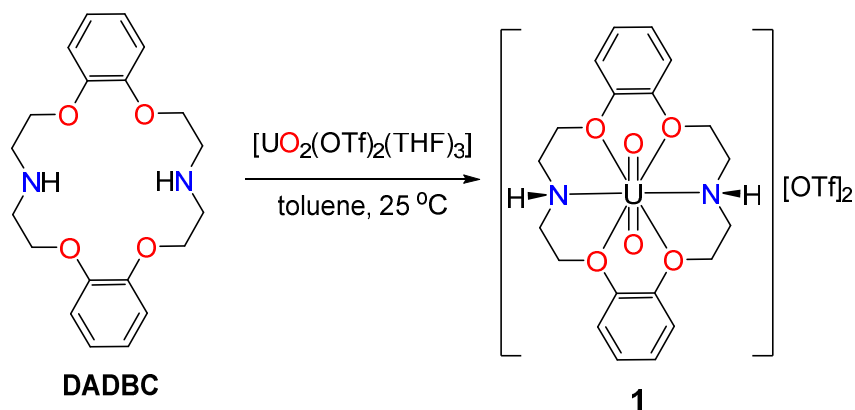
In an effort to expand the scope of uranyl macrocycle chemistry, we explored the reaction of $[\text{UO}_2(\text{OTf})_2(\text{THF})_3]$ with two macrocyclic ligands, the previously reported diaza-dibenzo-18-crown-6 (**DADBC**) and the novel 7,16-bis(*N*-methylacetamide)diaza-18-crown-6 (**BAM**). Both of these ligands are 18-membered macrocycles, for which different analogues have previously been shown to accommodate the linear UO_2^{2+} ion. **DADBC** was investigated in order to understand how rigidifying aromatic groups in the backbone can affect the complexation of UO_2^{2+} . Similarly, the new ligand **BAM** was synthesized to study how pendent donor groups on the diaza-18-crown-6 skeleton influence binding to UO_2^{2+} . Collectively, this work shows how these subtle factors can determine the likelihood that the linear UO_2^{2+} ion will “thread the needle” through a macrocyclic core.

Results and Discussion

Reaction of $[\text{UO}_2(\text{OTf})_2(\text{THF})_3]$ with 1 equiv of diaza-dibenzo-18-crown-6 (**DADBC**) in toluene results in a color change from yellow to orange. Workup of the reaction mixture, followed by crystallization from MeCN/Et₂O, results in isolation of $[\text{UO}_2(\text{DADBC})][\text{OTf}]_2$ (**1**) in 61% yield (Scheme 1). The room-temperature ¹H NMR spectrum of **1** in MeCN-*d*₃ features multiplets at 5.80, 5.18, 4.76, and 4.06 ppm, which are present in a 1:1:1:1 ratio. These resonances are assignable to four unique CH₂ environments of the dibenzo-diaza-18-crown-6 ligand and indicate that the ligand adopts a rigid saddle geometry in solution, which inhibits the exchange of axial and equatorial CH₂ environments. The spectrum also features multiplets at 7.64 and 7.38 ppm, in a 1:1 ratio, which are assignable to the two expected aryl

CH environments, along with a triplet at 6.98 ppm, which is assignable to the NH protons. For comparison, the ^1H NMR spectrum of $[\text{UO}_2(18\text{-crown-6})]^{2+}$ only features a single resonance, indicating stereochemical non-rigidity of the 18-crown-6 macrocycle.^[5] Surprisingly, the ^1H NMR spectrum of **1** in pyridine- d_5 features resonances attributable to free **DADBC** (Figure S11), demonstrating that strongly-donating, monodentate ligands can displace **DADBC** from the uranyl center.

The UV-Vis spectrum for **1**, recorded in MeCN, features an absorption at 463 nm ($390 \text{ M}^{-1}\cdot\text{cm}^{-1}$). The position and intensity of this resonance are typical of the uranyl moiety.^[59] For comparison, $[\text{UO}_2(18\text{-crown-6})]^{2+}$ exhibits an absorption at ca. 450 nm.^[5] The Raman spectrum of **1** features a strong, sharp vibration at 871 cm^{-1} , which we have assigned to the ν_1 mode. Also present in the spectrum is a weak, sharp vibration at 962 cm^{-1} , which we have tentatively assigned to the ν_3 mode. We hypothesize that the ν_3 mode, which is not usually Raman active, is observable because of the loss of the inversion center due to the saddle conformation of the **DADBC** macrocycle (see below).^[60-61] For comparison, the ν_1 and ν_3 modes of $[\text{UO}_2(\text{H}_2\text{O})_5]^{2+}$ are observed at 874 and 963 cm^{-1} , respectively.^[61-62] The similarity of these values with those of **1** suggests that **DADBC** is not a strong donor to uranyl, possibly because of a mismatch between its cavity size and the uranyl ionic radius. For further comparison, the ν_1 mode of $[\text{UO}_2(\text{Ph}_3\text{PO})_4][\text{OTf}]_2$ appears at 839 cm^{-1} , whereas the ν_1 mode of $[\text{UO}_2(\text{dppmo})_2(\text{OTf})][\text{OTf}]$ (dppmo = $\text{Ph}_2\text{P}(\text{O})\text{CH}_2\text{P}(\text{O})\text{Ph}_2$) appears at 848 cm^{-1} .^[63-64] Both values are substantially lower than that observed for **1**.



Scheme 1. Synthesis of complex **1**.

Complex **1** crystallizes in the monoclinic space group $C2/c$ as an acetonitrile and diethyl ether solvate, $1\cdot 2\text{MeCN}\cdot\text{Et}_2\text{O}$ (Figure 1). All six donor atoms of the macrocycle are ligated to the equatorial plane of the uranyl ion to provide a hexagonal bipyramidal coordination geometry. The structure also features two outer-sphere $[\text{OTf}]^-$ anions. The macrocycle ring adopts a saddle geometry, presumably to better accommodate the uranyl ion, consistent with the room temperature ^1H NMR data. The $\text{U}-\text{O}_{\text{yl}}$ distances ($1.768(4)$ and $1.765(4) \text{ \AA}$) and $\text{O}_{\text{yl}}-\text{U}-\text{O}_{\text{yl}}$ angle (180°) are typical of the uranyl ion.^[65-66] The $\text{U}-\text{O}_{\text{eq}}$ distances are $2.529(3)$ and $2.548(3) \text{ \AA}$, whereas the $\text{U}-\text{N}$ distance is $2.565(4) \text{ \AA}$. For comparison, the average $\text{U}-\text{O}_{\text{eq}}$ distance in $[\text{UO}_2(18\text{-crown-6})]^{2+}$ is $2.51(1) \text{ \AA}$ (range = $2.43(4)$ to $2.68(4) \text{ \AA}$),^[3] whereas the average $\text{U}-\text{O}_{\text{eq}}$ distance in $[\text{UO}_2(\text{H}_2\text{O})_5]^{2+}$ is $2.41(1) \text{ \AA}$ (range = $2.384(3)$ to $2.42(2) \text{ \AA}$).^[67] The latter $\text{U}-\text{O}_{\text{eq}}$ distance is notably shorter than that observed in **1**, perhaps because the oxygen donors in water are not constrained as they are within the macrocycle skeleton of **DADBC**. Also notable is the deviation of the two N-atoms from the uranyl equatorial plane (defined by $\text{U}1$, $\text{O}3$, $\text{O}4$, $\text{O}3^*$, and $\text{O}4^*$). In particular, $\text{N}1$ is

displaced from the equatorial plane by 0.361(6) Å. Such deviations are relatively rare, but have been observed in other uranyl macrocycle examples.^[52-53] This deviation is further evidence that uranyl does not fit well within the **DADBC** binding pocket. Finally, the N(1)–O_{OTf} distance (2.93 Å) is suggestive of the presence of a weak H-bond between the amide N-H protons and the outer-sphere triflate anions.

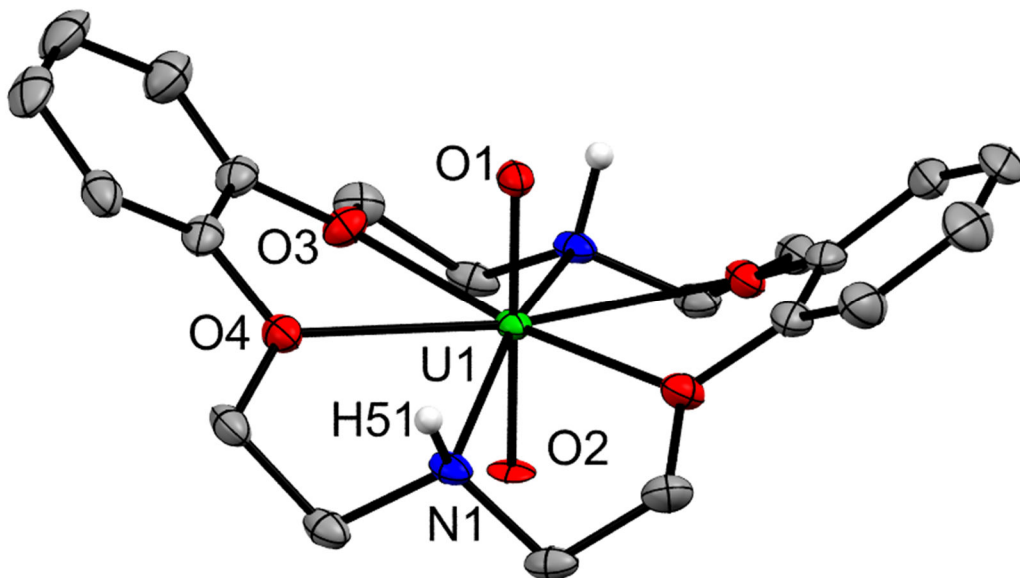
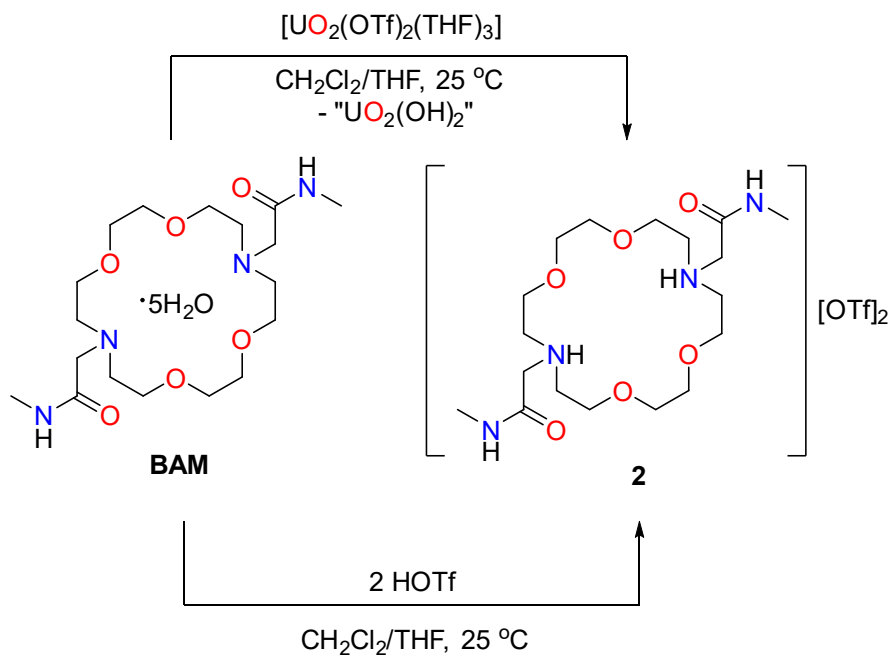


Figure 1. Solid-state molecular structure of **1**·2MeCN·Et₂O shown with 50% probability ellipsoids. Solvate molecules, triflate counterions, and hydrogen atoms are omitted for clarity. Selected bond lengths (Å) and angles (°): U1–O1 = 1.768(4), U1–O2 = 1.765(4), U1–O3 = 2.529(3), U1–N1 = 2.565(4), O1–U1–O2 = 180.0, O1–U1–O3 = 85.70(7), O3–U1–O4 = 59.80(10), N1–U1–N1* = 162.31(16), O3–U1–N1 = 120.18(11).

We also attempted to ligate uranyl with 7,16-bis(*N*-methylacetamide)diaza-18-crown-6 (**BAM**). Thus, layering a THF solution of [UO₂(OTf)₂(THF)₃] onto a CH₂Cl₂ solution of **BAM** results in the deposition of a pale yellow crystalline solid after standing for 3 d. Analysis of this material by X-ray crystallography reveals the formation of [H₂**BAM**][OTf]₂ (**2**), the doubly protonated form of the neutral macrocycle (Scheme 2). We hypothesize that **2** is formed by the reaction of [UO₂(OTf)₂(THF)₃] with **BAM**'s lattice H₂O molecules, which results in the formation of HOTf and UO₂(OH)₂. The former then protonates the amine groups of **BAM**, forming **2**. Not surprisingly, complex **2** can be made more conveniently by layering a THF solution of HOTf onto a CH₂Cl₂ solution of **BAM** (Scheme 2). When synthesized in this fashion, it can be isolated in 99% yield. The formation of **2** was confirmed by NMR spectroscopy. In particular, its ¹H NMR spectrum in DMSO-*d*₆ featured a broad resonance at 9.31 ppm, which was assigned to the two ammonium protons. Additionally, the ¹⁹F NMR spectrum exhibited a characteristic signal at –77.8 ppm, which reflects the presence of the triflate anions. The X-ray crystal structure of **2** also reveals the presence of the hydrogen atoms on the amine nitrogen atoms (Figure 2). The hydrogen atoms could be located on the difference Fourier map, and their presence is further supported by intramolecular hydrogen-bonding interactions with the pendent amide oxygen atoms, as evidenced by N···O distances of 2.64(7) and 2.67(7) Å. These values are in line with strong H-bonding interactions.^[68]



Scheme 2. Synthesis of compound **2**.

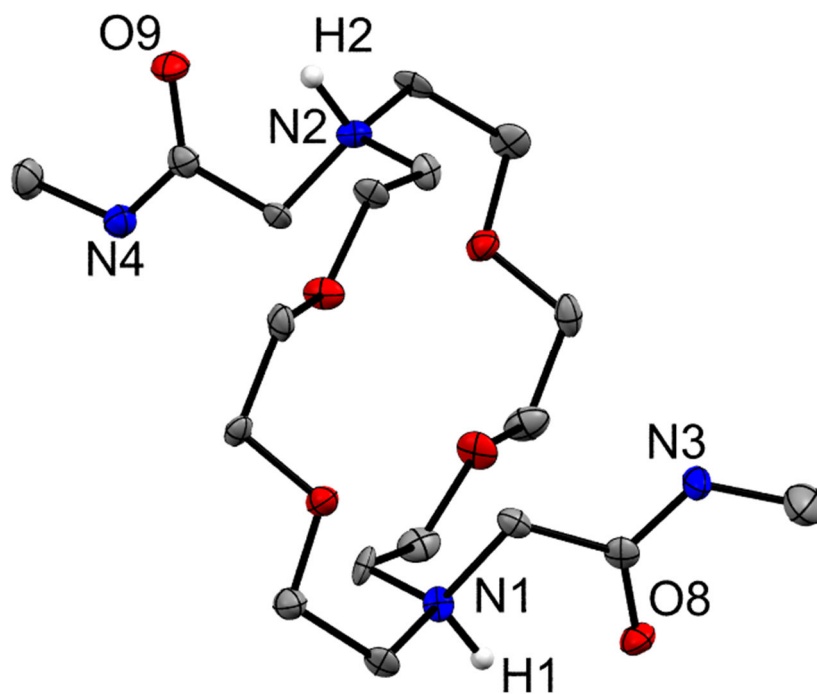
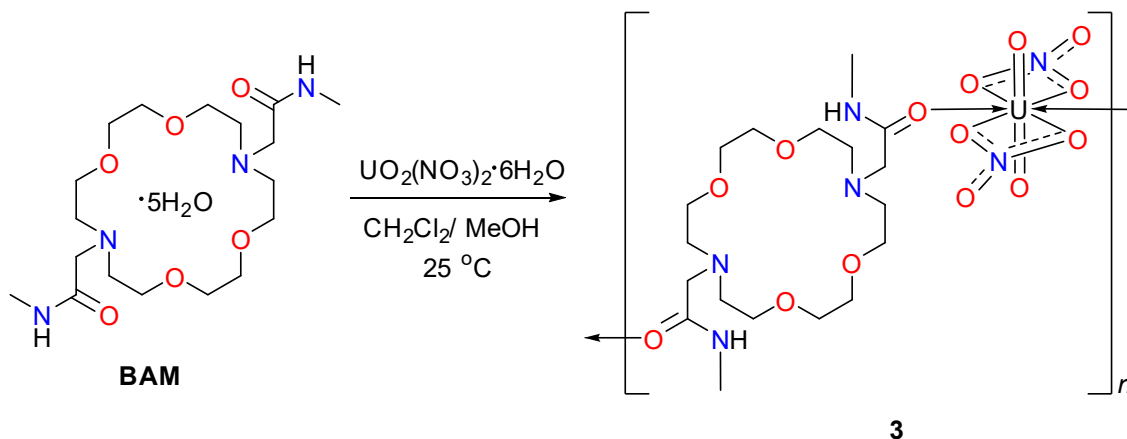


Figure 2. Solid-state molecular structure of **2** shown with 50% probability ellipsoids. Triflate anions and hydrogen atoms (except H1 and H2) are omitted for clarity. Selected bond lengths (Å): N1–O8 = 2.64 (7), N2–O9 = 2.67 (7).

We also investigated the complexation of uranyl nitrate with **BAM**. Thus, reaction of $UO_2(NO_3)_2 \cdot 6H_2O$ with 1 equiv of **BAM** in $CH_2Cl_2/MeOH$, followed by layering with pentane, results in the deposition of

$[\text{UO}_2(\kappa^2\text{-NO}_3)_2(\mu\text{-BAM})]_\infty$ (**3**) in 33% yield (Scheme 3). Complex **3** crystallizes in the monoclinic space group $P2_1/c$ as a one-dimensional coordination polymer. The macrocycle is centered on a crystallographic inversion center and maintains a conformation very similar to that observed in the structure of the free ligand (see below). Each pendent amide donor groups sit on opposite faces of the macrocycle, with the amide NH groups engaging in hydrogen bonds with the macrocycle tertiary amine ($\text{N1}\cdots\text{N2} = 2.658 \text{ \AA}$). The UO_2^{2+} ion, which also resides on a crystallographic inversion center, acts as a bridge between the neighboring macrocycles within the structure, as it interacts with the oxygen donors of the pendent carboxamides with a $\text{U}-\text{O}$ distance of $2.3782(12) \text{ \AA}$. For comparison, the closely-related $[\text{UO}_2(\kappa^2\text{-NO}_3)_2(\varepsilon\text{-caprolactam})_2]$ exhibits $\text{U}-\text{O}_{\text{caprolactam}}$ distance of $2.360(5) \text{ \AA}$,^[69] whereas $[\text{UO}_2(\kappa^2\text{-NO}_3)_2(2\text{-pyrrolidone})_2]$ exhibits an average $\text{U}-\text{O}_{\text{pyrrolidone}}$ distance of 2.38 \AA .^[70] In addition to these two carboxamide donors, the equatorial UO_2^{2+} coordination sphere is completed by two bidentate NO_3^- ligands, arranged *trans* relative to each other. The $\text{U}-\text{O}_{\text{NO}_3}$ distances in **3** ($2.5104(11)$ and $2.5443(15) \text{ \AA}$) are in good agreement with the $\text{U}-\text{O}_{\text{NO}_3}$ distances in previously reported $\text{UO}_2(\text{NO}_3)_2\text{L}_2$ -type complexes, which fall within a relatively narrow range (2.46 to 2.54 \AA).^[71-76] As expected, the UO_2^{2+} angle is perfectly linear (180°), as required by the crystallographic symmetry, and the $\text{U}-\text{O}$ distances are within the expected values ($1.7632(14) \text{ \AA}$).^[65-66] Complex **3** was also characterized by Raman spectroscopy. It features a strong vibration at 870 cm^{-1} , which we have assigned to the ν_1 mode. Not surprisingly, the ν_1 modes of $[\text{UO}_2(\kappa^2\text{-NO}_3)_2(\text{H}_2\text{O})_2]$ (876 cm^{-1}) and $[\text{K}][\text{UO}_2(\kappa^2\text{-NO}_3)_3]$ (871 cm^{-1}) are similar.^[60, 77-78]



Scheme 3. Synthesis of complex **3**.

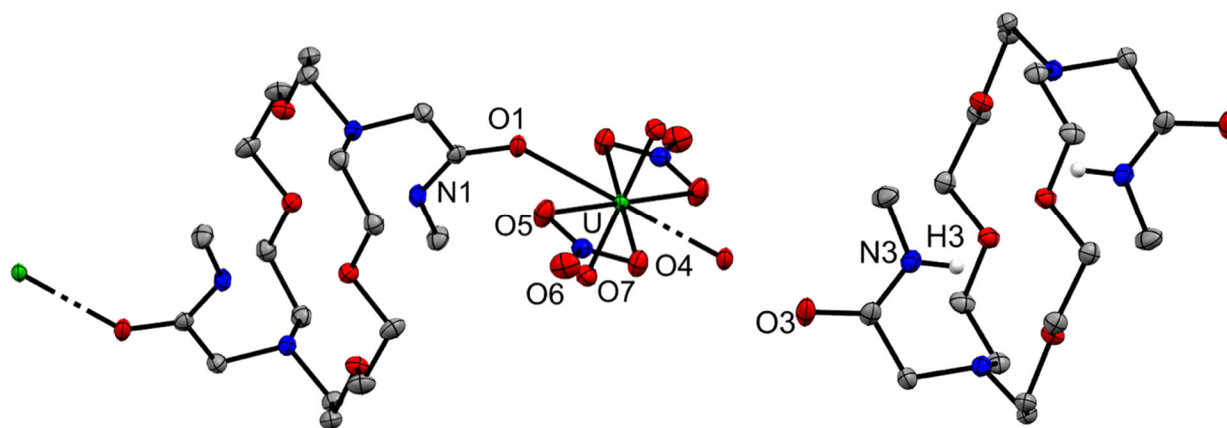


Figure 3. Solid-state molecular structures of **3** (left) and **BAM**·5H₂O (right) shown with 50% probability ellipsoids and hydrogen atoms are omitted for clarity. Selected bond lengths (Å) and angles (°): **3**: O1–U = 2.378(1), O5–U = 2.510(1), O4–U = 2.544(2), O7–U = 1.763(1), O7–U–O7* = 180. **BAM**·5H₂O: N2–N3 = 2.6736(15).

In an effort to understand the differing reactivity of **DADBC** and **BAM** with uranyl, we analyzed their solid-state structures by X-ray crystallography (see SI for full details). Interestingly, the **BAM** macrocycle crystallizes with five H₂O solvates, which rationalizes the origin of the ammonium protons in **2**. Additionally, the macrocycle ring and the two methylacetamide arms of free **BAM** adopt a closed “clamshell” configuration, which is identical to the conformation of the ligand seen in **3** (Figure 3). In particular, the amide H-bond distance in **BAM**·5H₂O (N2··N3 = 2.6736 (15) Å) is unchanged from the values observed for **3**. Overall, this comparison suggests that uranyl coordination within the **BAM** binding pocket is enthalpically unfavorable, due to the need to disrupt this closed conformation. As a result, coordination to uranyl only occurs via the amide oxygen (O1), which does not require rearrangement of the macrocycle skeleton. In contrast, the solid-state conformations of the **DADBC** macrocycle in its bound and free forms are similar (Figures 1 and S1), suggesting that uranyl coordination within the **DADBC** binding pocket requires minimal reorganization.

Conclusion

We have explored the reactivity of two aza-crown macrocycles, diaza-dibenzo-18-crown-6 (**DADBC**) and bis(*N*-methylacetamide)diaza-18-crown-6 (**BAM**), with the uranyl ion. Intriguingly, **DADBC** incorporates uranyl within its binding pocket (i.e., “threading the needle”), whereas **BAM** coordinates to uranyl, but not using its binding pocket. This difference is observed despite the fact that both ligands are 18-membered macrocycles. These complexes, along with the free macrocycles, were characterized by X-ray crystallography. This structural comparison shows that **DADBC** does not undergo a major conformation change upon uranyl binding. In contrast, the **BAM** macrocycle exhibits two intramolecular H-bonds in the solid state, whose cleavage is required for uranyl binding. However, it appears the uranyl coordination within the binding pocket cannot overcome this enthalpic penalty, so “threading the needle” does not occur. Overall, our results show that seemingly subtle changes in macrocycle structure can have a large effect on the reaction outcome. Macrocycle binding to uranyl is not necessarily straightforward, and the development of macrocycles for uranyl sensing or solvent extraction will need to consider these effects.

Appendix A. Supplementary data

CCDC contains the supplementary crystallographic data for **DADBC**, **BAM**, **1**, **2**, and **3**. These data can be obtained free of charge via <http://www.ccdc.cam.ac.uk/conts/retrieving.html>, or from the Cambridge Crystallographic Data Centre, 12 Union Road, Cambridge CB2 1EZ, UK; fax: (+44) 1223-336-033; or e-mail: deposit@ccdc.cam.ac.uk.

Supporting Information. Experimental procedures, crystallographic details, and spectral data for **DADBC**, **BAM**, **1**, **2**, and **3** (PDF).

AUTHOR INFORMATION

Corresponding Author

*hayton@chem.ucsb.edu, justinwilson@ucsb.edu

Author Contributions

The manuscript was written through contributions of all authors. All authors have given approval to the final version of the manuscript.

ACKNOWLEDGMENT

This work was supported by the U.S. Department of Energy, Office of Basic Energy Sciences, Chemical Sciences, Biosciences, and Geosciences Division under Contract DE-SC0001861, and by the National Institutes of Health under award number R56 EB029259.

References

- [1] T. W. Hayton, *Dalton Trans.* **2018**, 47, 1003-1009.
- [2] D. R. Hartline, S. T. Löffler, D. Fehn, J. M. Kasper, F. W. Heinemann, P. Yang, E. R. Batista, K. Meyer, *J. Am. Chem. Soc.* **2023**, 145, 8927-8938.
- [3] A. Navaza, F. Villain, P. Charpin, *Polyhedron* **1984**, 3, 143-149.
- [4] P. Thuery, N. Keller, M. Lance, *New J. Chem.* **1995**, 19, 619-625.
- [5] G. Folcher, P. Charpin, R.-M. Costes, N. Keller, G. C. d. Villardi, *Inorg. Chim. Acta* **1979**, 34, 87-90.
- [6] M. Brighli, P. Fux, J. Lagrange, P. Lagrange, *Inorg. Chem.* **1985**, 24, 80-84.
- [7] P. Fux, J. Lagrange, P. Lagrange, *J. Am. Chem. Soc.* **1985**, 107, 5927-5931.
- [8] A. DEJEAN, P. CHARPIN, G. FOLCHER, P. RIGNY, A. NAVAZA, G. TSOUCARIS, *J. Phys. Colloques* **1986**, 47, 645648.
- [9] T. Gutberlet, W. Dreissig, P. Luger, H.-C. Bechthold, R. Maung, A. Knochel, *Acta Crystallograph., Sect. C* **1989**, 45, 1146-1149.
- [10] J. Lagrange, J.-P. Metabanzoulou, P. Lagrange, *J. Chim. Phys.* **1989**, 86, 1369-1367.
- [11] C. Yonezawa, G. R. Choppin, *J. Radioanal. Nucl. Chem.* **1989**, 134, 233-239.
- [12] J. Lagrange, J. P. Metabanzoulou, P. Fux, P. Lagrange, *Polyhedron* **1989**, 8, 2251-2254.
- [13] P. Thuery, N. Keller, M. Lance, J.-M. Sabattie, J.-D. Vigner, M. Nierlich, *Acta Crystallograph., Sect. C* **1995**, 51, 801-805.
- [14] J. M. Harrowfield, M. I. Ogden, A. H. White, *J. Chem. Soc., Dalton Trans.* **1991**, 979-985.
- [15] M. M. Pynch, R. L. Meyer, T. Rajeshkumar, P. A. Cooke, D. J. Fiszbein, E. Ito, N. J. Katzer, C. S. Conour, S. G. Minasian, L. Maron, P. L. Arnold., *Angew. Chem. Int. Ed.* **2025**, 64, e202422974.
- [16] Z. Asfari, A. Bilyk, J. W. C. Dunlop, A. K. Hall, J. M. Harrowfield, M. W. Hosseini, B. W. Skelton, A. H. White, *Angew. Chem. Int. Ed.* **2001**, 40, 721-723.
- [17] A. K. Burrell, G. Hemmi, V. Lynch, J. L. Sessler, *J. Am. Chem. Soc.* **1991**, 113, 4690-4692.
- [18] J. L. Sessler, T. D. Mody, V. Lynch, *Inorg. Chem.* **1992**, 31, 529-531.
- [19] J. L. Sessler, S. J. Weghorn, Y. Hiseada, V. Lynch, *Chem. Eur. J.* **1995**, 1, 56-67.
- [20] J. L. Sessler, A. Gebauer, *Chem. Commun.* **1998**, 1835-1836.
- [21] J. L. Sessler, D. Seidel, C. Bucher, V. Lynch, *Tetrahedron* **2001**, 57, 3743-3752.
- [22] J. L. Sessler, D. Seidel, A. E. Vivian, V. Lynch, B. L. Scott, D. W. Keogh, *Angew. Chem. Int. Ed.* **2001**, 40, 591-594.
- [23] J. L. Sessler, A. E. Vivian, D. Seidel, A. K. Burrell, M. Hoehner, T. D. Mody, A. Gebauer, S. J. Weghorn, V. Lynch, *Coord. Chem. Rev.* **2001**, 216-217, 411-434.
- [24] J. L. Sessler, A. E. V. Gorden, D. Seidel, S. Hannah, V. Lynch, P. L. Gordon, R. J. Donohoe, C. Drew Tait, D. Webster Keogh, *Inorg. Chim. Acta* **2002**, 341, 54-70.
- [25] G. M. Jones, P. L. Arnold, J. B. Love, *Chem. Eur. J.* **2013**, 19, 10287-10294.
- [26] P. L. Arnold, E. Hollis, G. S. Nichol, J. B. Love, J.-C. Griveau, R. Caciuffo, N. Magnani, L. Maron, L. Castro, A. Yahia, S. O. Odoh, G. Schreckenbach, *J. Am. Chem. Soc.* **2013**, 135, 3841-3854.
- [27] G. M. Jones, P. L. Arnold, J. B. Love, *Angew. Chem. Int. Ed.* **2012**, 51, 12584-12587.
- [28] P. L. Arnold, G. M. Jones, S. O. Odoh, G. Schreckenbach, N. Magnani, J. B. Love, *Nat. Chem.* **2012**, 4, 221-227.
- [29] P. L. Arnold, A.-F. Pécharman, J. B. Love, *Angew. Chem. Int. Ed.* **2011**, 50, 9456-9458.
- [30] P. L. Arnold, E. Hollis, F. J. White, N. Magnani, R. Caciuffo, J. B. Love, *Angew. Chem. Int. Ed.* **2011**, 50, 887-890.
- [31] A. Yahia, P. L. Arnold, J. B. Love, L. Maron, *Chem. Eur. J.* **2010**, 16, 4881-4888.
- [32] P. L. Arnold, A.-F. Pecharman, E. Hollis, A. Yahia, L. Maron, S. Parsons, J. B. Love, *Nat. Chem.* **2010**, 2, 1056-1061.
- [33] P. L. Arnold, D. Patel, C. Wilson, J. B. Love, *Nature* **2008**, 451, 315-318.

- [34] P. L. Arnold, D. Patel, A. J. Blake, C. Wilson, J. B. Love, *J. Am. Chem. Soc.* **2006**, *128*, 9610-9611.
- [35] P. L. Arnold, A. J. Blake, C. Wilson, J. B. Love, *Inorg. Chem.* **2004**, *43*, 8206-8208.
- [36] A. Kumar, D. Lionetti, V. W. Day, J. D. Blakemore, *J. Am. Chem. Soc.* **2020**, *142*, 3032-3041.
- [37] R. R. Golwankar, A. C. Ervin, M. Z. Makoś, E. R. Mikeska, V.-A. Glezakou, J. D. Blakemore, *J. Am. Chem. Soc.* **2024**, *146*, 9597-9604.
- [38] A. Kumar, R. R. Golwankar, M. M. F. Pynch, F. L. Cooper, G. A. Arehart, K. P. Carter, A. G. Oliver, V. W. Day, T. Z. Forbes, J. D. Blakemore, *Dalton Trans.* **2025**, *54*, 8061-8075.
- [39] G. A. Shamov, G. Schreckenbach, R. L. Martin, P. J. Hay, *Inorg. Chem.* **2008**, *47*, 1465-1475.
- [40] G. A. Shamov, G. Schreckenbach, *Inorg. Chem.* **2008**, *47*, 805-811.
- [41] P. Guilbaud, G. Wipff, *J. Phys. Chem.* **1993**, *97*, 5685-5692.
- [42] P. Guilbaud, G. Wipff, *J. inclusion phenom. mol. recognit. chem.* **1993**, *16*, 169-188.
- [43] M. Yang, W. Ding, D. Wang, *New J. Chem.* **2017**, *41*, 63-74.
- [44] M.-S. Liao, T. Kar, S. Scheiner, *J. Phys. Chem. A* **2004**, *108*, 3056-3063.
- [45] O. A. Gerasko, D. G. Samsonenko, A. A. Sharonova, A. V. Virovets, J. Lipkowski, V. P. Fedin, *Russ. Chem. Bull.* **2002**, *51*, 346-349.
- [46] R. D. Rogers, M. M. Benning, *J. inclusion phenom. mol. recognit. chem.* **1991**, *11*, 121-135.
- [47] J. Jian, S.-X. Hu, W.-L. Li, M. J. van Stipdonk, J. Martens, G. Berden, J. Oomens, J. Li, J. K. Gibson, *Inorg. Chem.* **2018**, *57*, 4125-4134.
- [48] S.-X. Hu, J. K. Gibson, W.-L. Li, M. J. Van Stipdonk, J. Martens, G. Berden, B. Redlich, J. Oomens, J. Li, *Chem. Commun.* **2016**, *52*, 12761-12764.
- [49] Y. Gong, J. K. Gibson, *Inorg. Chem.* **2014**, *53*, 5839-5844.
- [50] R. D. Rogers, M. M. Benning, R. D. Etzenhouser, A. N. Rollins, *J. Coord. Chem.* **1992**, *26*, 299-311.
- [51] R. D. Rogers, M. M. Benning, R. D. Etzenhouser, A. N. Rollins, *J. Chem. Soc., Chem. Commun.* **1989**, 1586-1588.
- [52] E. A. Pedrick, J. W. Schultz, G. Wu, L. M. Mirica, T. W. Hayton, *Inorg. Chem.* **2016**, *55*, 5693-5701.
- [53] G. T. Kent, J. Murillo, G. Wu, S. Fortier, T. W. Hayton, *Inorg. Chem.* **2020**, *59*, 8629-8634.
- [54] M. K. Assefa, E. A. Pedrick, M. E. Wakefield, G. Wu, T. W. Hayton, *Inorg. Chem.* **2018**, *57*, 8317-8324.
- [55] E. A. Pedrick, M. K. Assefa, M. E. Wakefield, G. Wu, T. W. Hayton, *Inorg. Chem.* **2017**, *56*, 6638-6644.
- [56] R. D. Rogers, L. K. Kurihara, M. M. Benning, *J. inclusion phenom.* **1987**, *5*, 645-658.
- [57] J. A. Danis, M. R. Lin, B. L. Scott, B. W. Eichhorn, W. H. Runde, *Inorg. Chem.* **2001**, *40*, 3389-3394.
- [58] R. D. Rogers, A. H. Bond, W. G. Hipple, A. N. Rollins, R. F. Henry, *Inorg. Chem.* **1991**, *30*, 2671-2679.
- [59] E. Rabinowitch, R. L. Belford, *Spectroscopy and Photochemistry of Uranyl Compounds*, Macmillan, New York, **1964**.
- [60] G. Lu, A. J. Haes, T. Z. Forbes, *Coord. Chem. Rev.* **2018**, *374*, 314-344.
- [61] G. Lu, T. Z. Forbes, A. J. Haes, *Anal. Chem.* **2016**, *88*, 773-780.
- [62] M. Gál, P. L. Goggin, J. Mink, *J. Mol. Struct.* **1984**, *114*, 459-462.
- [63] E. A. Pedrick, G. Wu, T. W. Hayton, *Inorg. Chem.* **2015**, *54*, 7038-7044.
- [64] S. M. Cornet, I. May, M. P. Redmond, A. J. Selvage, C. A. Sharrad, O. Rosnel, *Polyhedron* **2009**, *28*, 363-369.
- [65] S. Fortier, T. W. Hayton, *Coord. Chem. Rev.* **2010**, *254*, 197-214.
- [66] R. G. Denning, *J. Phys. Chem. A* **2007**, *111*, 4125-4143.
- [67] L. Deshayes, N. Keller, M. Lance, M. Nierlich, J.-D. Vigner, *Acta Crystallograph., Sect. C* **1994**, *50*, 1541-1544.
- [68] T. C. Johnstone, E. M. Nolan, *J. Am. Chem. Soc.* **2017**, *139*, 15245-15250.
- [69] Z. Cao, H. Wang, J. Gu, L. Zhu, K. Yu, *Acta Crystallograph., Sect. C* **1993**, *49*, 1942-1943.

- [70] K. Takao, K. Noda, Y. Morita, K. Nishimura, Y. Ikeda, *Cryst. Growth Des.* **2008**, *8*, 2364-2376.
- [71] G. Agostini, G. Giacometti, D. A. Clemente, M. Vicentini, *Inorg. Chim. Acta* **1982**, *62*, 237-240.
- [72] R. Babecki, A. W. G. Platt, J. C. Tebby, J. Fawcett, D. R. Russell, R. Little, *Polyhedron* **1989**, *8*, 1357-1360.
- [73] D. Das, M. Joshi, S. Kannan, M. Kumar, T. K. Ghanty, T. Vincent, S. Manohar, C. P. Kaushik, *Polyhedron* **2019**, *171*, 486-492.
- [74] C. Berger, C. Marie, D. Guillaumont, C. Tamain, T. Dumas, T. Dirks, N. Boubals, E. Acher, M. Laszczyk, L. Berthon, *Inorg. Chem.* **2020**, *59*, 1823-1834.
- [75] D. L. Perry, H. Ruben, D. H. Templeton, A. Zalkin, *Inorg. Chem.* **1980**, *19*, 1067-1069.
- [76] D. Das, S. Kannan, D. K. Maity, M. G. B. Drew, *Inorg. Chem.* **2012**, *51*, 4869-4876.
- [77] P. K. Khulbe, R. Ttripathi, H. D. Bist, *J. Phys. Chem. Solids* **1992**, *53*, 639-650.
- [78] J. I. Bullock, *J. Inorg. Nucl. Chem.* **1967**, *29*, 2257-2264.